Supporting Information on:

Computational analysis of the effect of [TEA][Ms] and $[TEA][H_2PO_4]$ ionic liquids on the structure and stability of $A\beta(17-42)$ amyloid fibrils

D. Gobbo,[(1)] A. Cavalli,[(1,2)], P. Ballone,[(3,4)] A. Benedetto[(3,4,5,6)]

(1) Computational and Chemical Biology,

Fondazione Istituto Italiano di Tecnologia, Genova, Italy

(2) University of Bologna, Bologna, Italy

(3) School of Physics, University College, Dublin, Ireland

(4) Conway Institute for Biomolecular and Biomedical

Research, University College, Dublin, Ireland

(5) Department of Sciences, University of Roma Tre, Rome, Italy and

(6) Laboratory for Neutron Scattering,

Paul Scherrer Institute, Villigen, Switzerland

I. DENSITY FUNCTIONAL COMPUTATIONS FOR THE SINGLE IONS AND NEUTRAL ION PAIRS

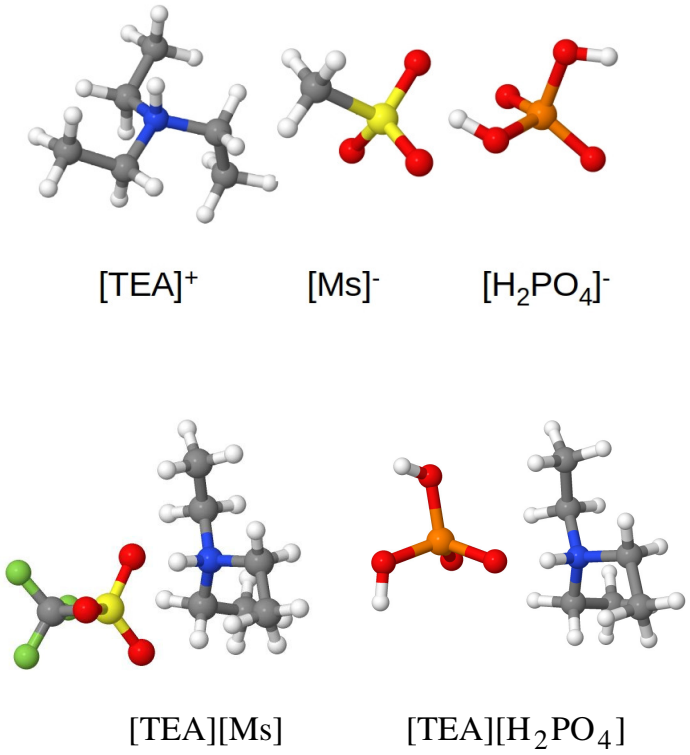

FIG. S1: Ground state structure for the isolated ions and neutral ion pairs considered in our simulations. Geometries optimised by quench molecular dynamics using the CPMD code.[1]

The geometry and electronic structure of the single ions $[Tea]^+$, $[Ms]^-$, $[H_2PO_4]^-$ and neutral ion pairs [Tea][Ms] and $[Tea][H_2PO_4]$ have been determined by density functional approaches to provide a preliminary validation of the force field used in our molecular dynamics simulations.

All density functional computations have been carried out within the pseudopotential - plane wave framework, implemented in the CPMD computer package.[1] Soft norm-conserving pseudopotentials have bee used,[2] expanding orbitals on a plane wave basis set with a kinetic energy cut off of 90 Ry. The PBE exchange-correlation energy[3] has been used, ad charged systems have been treated with a suitable approach excluding the Coulomb interaction with periodic replicas.[4]

The results for the geometry, the vibrational modes and the RESPA atomic charges have been compared to the corresponding quantities in the force field approach, finding fair agreement, in line with the same comparison for the other RTIL systems we simulated in the past.

II. HOFMEISTER ORDERING OF [TEA][MS] AND [TEA][H_2PO_4] PROTIC IONIC LIQUIDS IN WATER

The kosmotropic or chaotropic character of an ionic compound is traditionally explained in terms of its perturbation of the hydrogen bonding network of water,[5] hence we first compute the average number $\langle n_{hb} \rangle$ of H-bonds shared by each water molecule with other water molecules. In principle, the analysis of the salt effect on the H-bonding of water should be carried out at low salt concentration, before the saturation of donor and acceptor sites of water by the ions brings about a generalised decrease of water-water H-bonding. However, we will rely also on the comparison of samples at the same ionic strength to rank different salts over a wider concentration range. Comparison of the result for control-[Na][Cl] and 3%-[Tea][Ms] (see Tab. S1) shows that, at low concentration, [Tea][Ms] increases, although slightly, the number of H-bonds among water molecules. In an intuitive interpretation of kosmotropic character as enhancing the hydrogen bonding of water, [Tea][Ms] appears as structure forming or kosmotropic. At the equivalent salt concentration of 25%-[Tea][Ms] and 26%-[Tea][H_2PO_4], [Tea][H_2PO_4] perturbs the H-bonds network of water slightly less than [Tea][Ms], appearing as the most kosmotropic of the two compounds, in agreement with the ordering assumed in Ref. 6. However, both the variation of $\langle n_{hb} \rangle$ with respect to the control sample control-[Na][Cl] and the difference between the [Tea][Ms] and [Tea][H_2PO_4] samples are minor at least up to ~ 25 wt% concentration.

Since the connection of the average number $\langle n_{hb} \rangle$ with kosmotropic and chaotropic behaviour is not so obvious, we follow Ref. 7, and determine a second index. First, for each water molecule i, we compute the ratio:

$$\theta_i = n^i_{hb}/n^i_{neigh}$$

where n^i_{neigh} is the number of neighbouring water molecules within the H-bonding cut off $r_c = 3.2$ Å , and n^i_{hb} is the number of these neighbouring molecules forming an H-bond with

TABLE S1: Average number per water molecule $\langle n_{hb} \rangle$ of H-bonds shared among water molecules. H-bonds OW-H—OW are defined by a distance $d[OW - OW] \leq r_c = 3.2$ Å , and $OW - \widehat{H} - OW$ angle deviating less than 30° from linearity. The parameter $\langle \theta \rangle$ measuring kosmotropic versus chaotropic character is defined in the text. The statistical error bar is implicitly given by the number of digits reported in the table.

	control-[Na][Cl]	3%-[Tea][Ms]	11%-[Tea][Ms]	25%-[Tea][Ms]	88%-[Tea][Ms]	26%-[Tea][H_2PO_4]
$\langle n_{hb} \rangle$	1.41	1.42	1.39	1.34	0.57	1.37
$\langle \theta \rangle$	0.731	0.739	0.747	0.763	0.716	0.755

the central molecule i, according to the definition of Tab. S1. Then, the index $\langle \theta \rangle$ is the average of θ_i over all water molecules and over all configurations collected for each sample. The index $\langle \theta \rangle$ goes beyond the information given by the average $\langle n_{hb} \rangle$ since it accounts also for the correlation of n_{hb}^i with the local packing of water molecules. The results for $\langle \theta \rangle$ are given again in Tab. S1. According to the calibration of Ref. 7, [Tea][Ms] is chaotropic, since its $\langle \theta \rangle$ index exceeds the value of the control sample control-[Na][Cl], contradicting the result based on $\langle n_{hb} \rangle$. Comparison of $\langle \theta \rangle$ for [Tea][Ms] and [Tea][H_2PO_4] at ~ 25 wt% (25%-[Tea][Ms] and 26%-[Tea][H_2PO_4]), however, shows that [Tea][H_2PO_4] is slightly less chaotropic, or more kosmotropic, than [Tea][Ms], in agreement with the assessment based on $\langle n_{hb} \rangle$ and with the ranking assumed in the experimental Ref. 6.

It is apparent that, at the atomistic simulation scale, determining the Hofmeister ordering is difficult, especially for organic salts.[5] More importantly, the predictive power of this concept is uncertain. In the case of Aβ fibrillation, for instance, its following of a direct or an inverse Hofmeister ordering[6] is a purely empirical statement, which, to the best of our knowledge, cannot be derived from a-priori understanding.

Last but not least, the application of the Hofmeister series concept to this case suffers from a further problem of interpretation, since one has to decide whether the *folded state* whose stability is affected by the salt is the *native*, random coil-like state of the single peptide in solution, or it is the amyloid state, which is in fact folded into a well defined configuration, has low energy and has low propensity for further aggregation.

III. PEPTIDE CONFIGURATION AT THE END OF THE UMBRELLA SAMPLING COMPUTATION

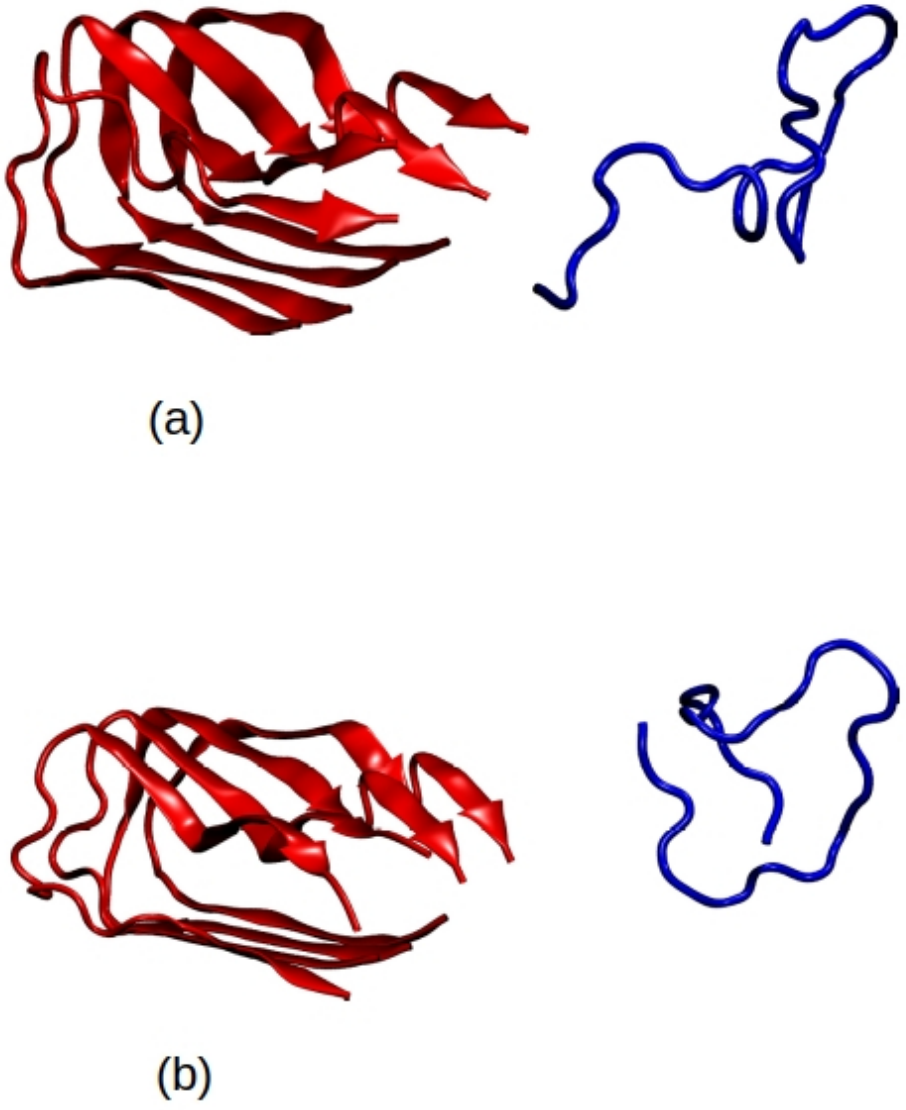

FIG. S2: Peptide configuration at the end of the umbrella sampling stage. The two figures refer to the last (31st) window of umbrella sampling. Panel (a): 4-peptide fibril and solvated peptide in 25wt%-[Tea][Ms]; panel (b): 4-peptide fibril and solvated peptide in 26wt%-[Tea][H_2PO_4]. The orientation of each sample has been optimized to display the two parts as distinct but close to each other.

IV. WATER AND IONS HYDROGEN BONDING IN THE SOLUTION OF THE SIMULATED SAMPLES

TABLE S2: Average number of H-bonds in the RTIL/water solution of the simulated systems. The numbers report averages for the whose sample, whose composition is specified in Tab. I of the main text. The arrow indicates the direction of the proton donation in the H-bonds. The number of digits is consistent with the error bar.

Property	control-[Na][Cl]	3%-[Tea][Ms]	11%-[Tea][Ms]	25%-[Tea][Ms]	88%-[Tea][Ms]	26%-[Tea][H_2PO_4]
Water → Water	15060	15070	14510	10850	910	11090
Cation → Water	0	23.5	97.7	192	543	33.3
Water → Anion	46	98.7	550	1070	1803	679
Anion → Water	0	0.0	0	0.0	0	13.3
Cation → Anion	0	0.4	2.6	0.5	200	183
Anion → Anion	0	0.0	0	0.0	0	0.04

V. NANO-STRUCTURING IN THE 25%-[TEA][MS] SOLUTION

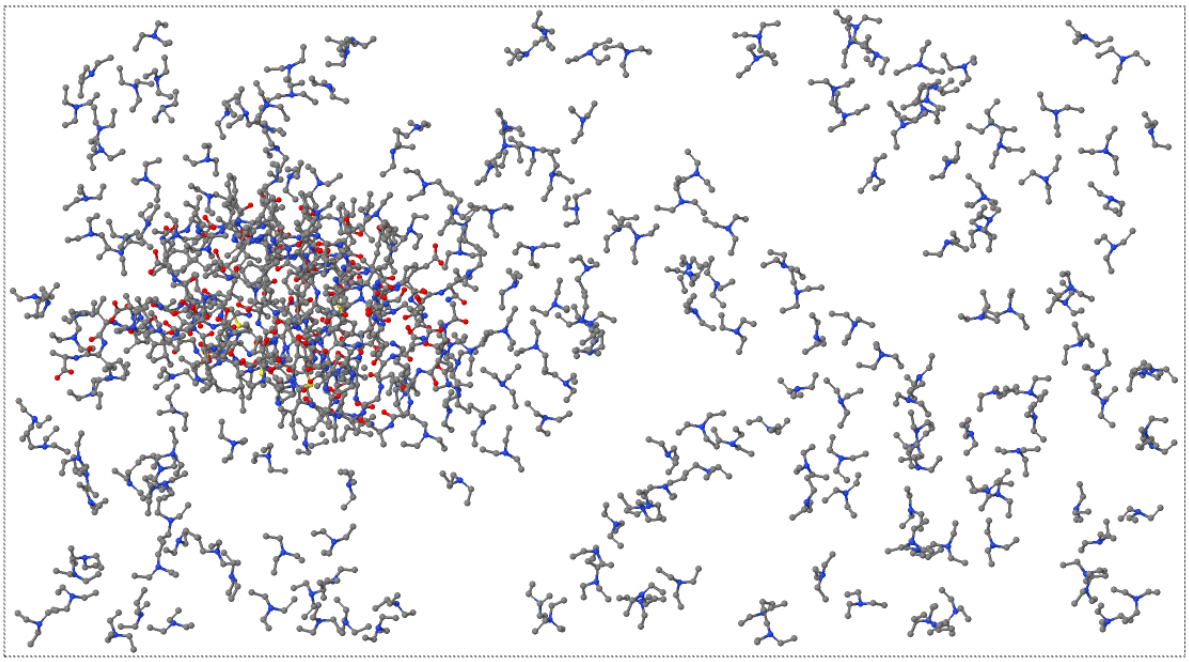

FIG. S3: Simulation snapshot of 25%-[Tea][Ms]. For the sake of clarity, only the protofibril and the cations are reported, and all hydrogen atoms have been removed. Nanometric fluctuations in the ion distribution give origin to wide volumes devoid of cations. The protofibril represents an aggregation centre for the RTIL.

VI. FLOW-LIKE DIFFUSION OF $[TEA]^+$ AND $[MS]^-$ IN 88%-[TEA][MS]

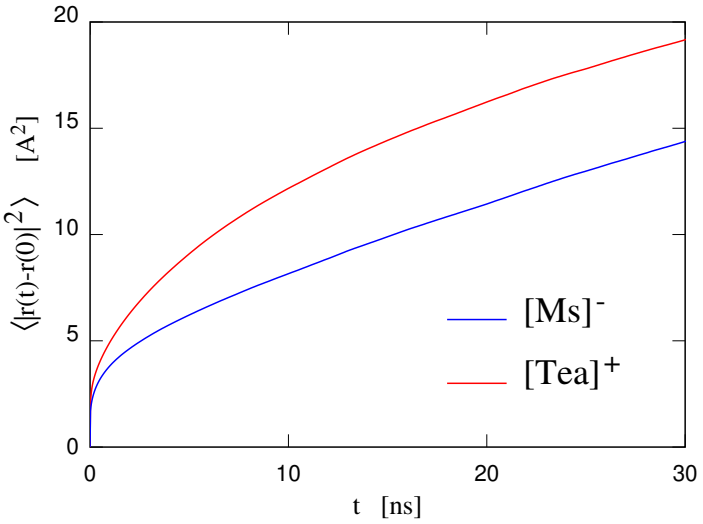

FIG. S4: Mean square displacement as a function of time of $[Tea]^+$ and $[Ms]^-$ in 88%-[Tea][Ms]. Despite the high [Tea][Ms] concentration (88 wt%), the diffusion of the ions, although slow, is flow-like and not jump-like.

VII. THE OVERALL PROTOFIBRIL GEOMETRY

The nearly constant overall shape and size of the protofibril in all cases and over the entire simulation times suggests to first analyse the protofibril as an elastic body. This has been done by computing the principal momenta of inertia (I_{xx}, I_{yy}, I_{zz}) as a function of time. For a more immediate interpretation in terms of size and shape, these momenta have been converted into the a, b and c radii of the ellipsoid $x^2/a^2 + y^2/b^2 + z^2/c^2 = k^2$ of homogeneous density and mass equal to the peptide mass, approximating the protofibril shape using the relations:

$$a^2 = \frac{5}{2M}\left(I_{yy} + I_{zz} - I_{xx}\right)$$
$$b^2 = \frac{5}{2M}\left(I_{xx} + I_{zz} - I_{yy}\right)$$
$$c^2 = \frac{5}{2M}\left(I_{xx} + I_{yy} - I_{zz}\right)$$

from which a volume can be attributed to the protofibril through $Vol = 4\pi abc/3$. The average values of a, b and c are given in Tab. S3 of the main text for all the samples. Standard deviations are given as well, since the elastic moduli of the protofibril could be computed from average values and their standard deviation.

The orientation of the protofibril with respect to the reference frame identified by the principal axes of inertia is illustrated in Fig. S5.

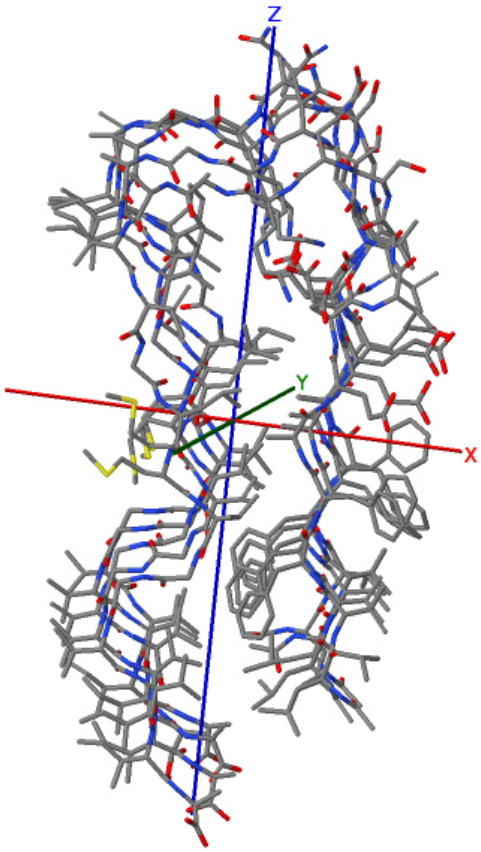

FIG. S5: Typical orientation of the protofibril with respect to the principal axes of inertia (x, y, z). Snapshot from the simulation of 25%-[Tea][Ms].

The analysis of several snapshots shows that the orientation of the protofibril with respect to the principal axes of inertia is simple, as shown in Fig. S5.

The changes in the radii and in volume due to the salt addition are small, but the increase of the protofibril volume in 25%-[Tea][Ms] and especially in 26%-[Tea][H_2PO_4] (See Tab. S3) is well above the error bar, and is accompanied, or perhaps caused, by a limited penetration

TABLE S3: Radii a, b and c of the ellipsoid of homogeneous density approximating the protofibril shape (see text). Their standard deviation δa, δb and δc are reported as well. All lengths are in Å , the volume of the ellipsoid is in Å ^{3}. Because of the short auto-correlation time, the statistical error on the gyration radii is an order of magnitude smaller than δa, δb, δc. The protofibril orientation with respect to the principal axes of inertia is shown in Fig. S5. The lowest radius, here called a, corresponds the thickness of the double strand structure. The product of b and c is the area covered by the two sheets. The number of significant digits is consistent with the estimated error bars.

Sample	a	δa	b	δb	c	δc	Vol
control-[Na][Cl]	11.83	0.15	16.30	0.12	24.62	0.17	19880
3%-[Tea][Ms]	11.88	0.18	16.18	0.13	24.73	0.20	19920
11%-[Tea][Ms]	12.12	0.23	16.22	0.13	24.66	0.22	20310
25%-[Tea][Ms]	11.98	0.20	16.62	0.20	24.68	0.20	20575
88%-[Tea][Ms]	11.89	0.10	16.44	0.10	24.67	0.12	20190
26%-[Tea][H_2PO_4]	12.66	0.23	17.19	0.20	23.53	0.23	21450

of water (but not of ions) into the concave side of the U-shaped fibril. The high viscosity of 88%-[Tea][Ms], due to the high [Tea][Ms] concentration in this sample, limits the variation in the protofibril shape, bringing a, b, c back to their control-[Na][Cl] values, and reduces significantly δa, δb, δc.

VIII. SECONDARY STRUCTURE

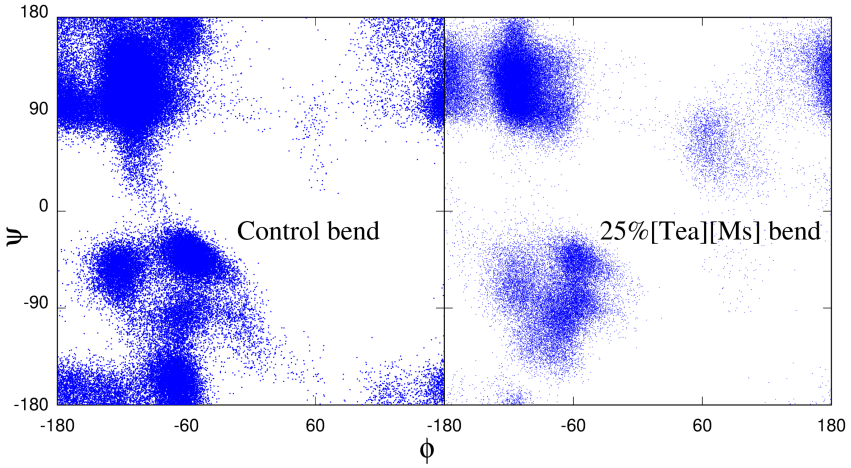

FIG. S6: Ramachandran plot of the bend segment in control-[Na][Cl] and 25%-[Tea][Ms]

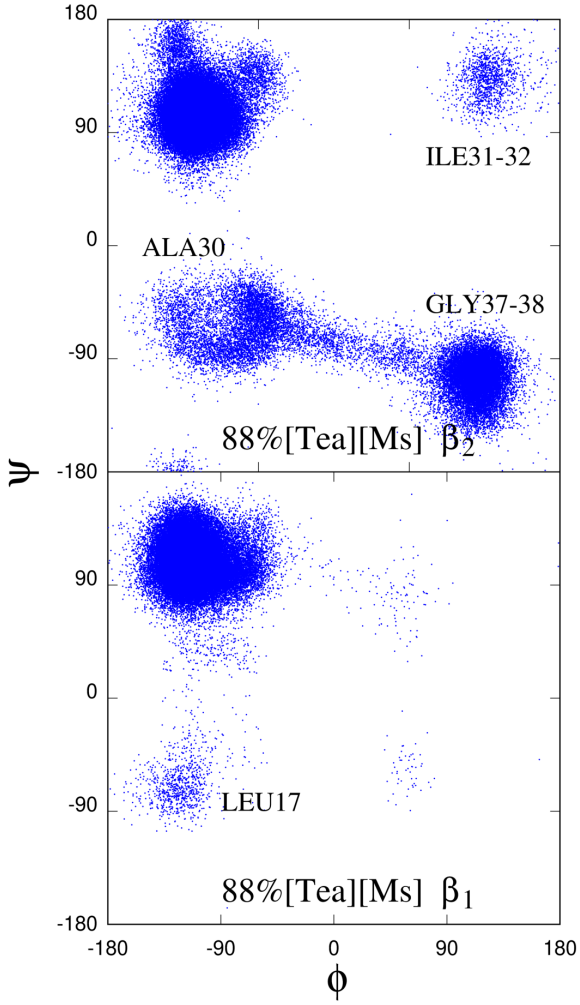

FIG. S7: Ramachandran plot for the β_1 and the β_2 segment in 88%-[Tea][Ms]

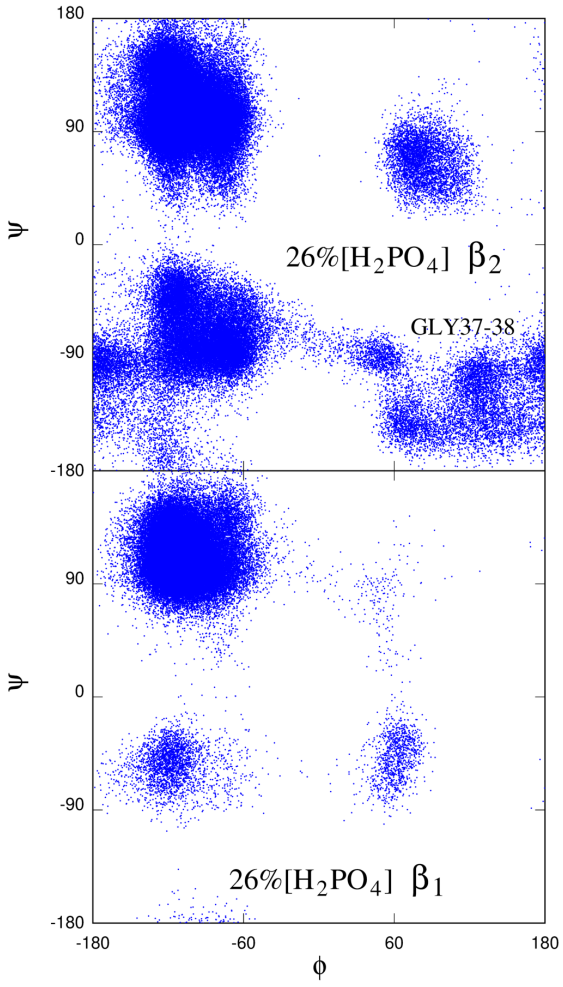

FIG. S8: Ramachandran plot for the β_1 and the β_2 segment in 26%-[Tea][H_2PO_4]

IX. PEPTIDE HYDROGEN BONDING

A major player in the determination of the protofibril secondary structure is the distribution of H-bonds accepted and donated by each peptide to other peptides, to water and to the ions, whose detailed account is given in Tab. IV. Each Aβ peptide has 26 proton donors and 26 acceptors along its backbone, including the carbonyl group ACE1 and excluding the COO^- on the ALA42 termination. A few extra-backbone acceptors and donors are present. In all samples, virtually no intra-peptide bond is present, apparently for conformational constraints due to the protofibril structure. The only noticeable exception is the salt bridge

that is discussed below.

At any given time, slightly more than 200 H-bonds are formed in control-[Na][Cl] by the peptides of the protofibril, representing more than 75% of the full H-bonding capacity. In this analysis, peptide-peptide H-bonds are counted twice, since they saturate both an acceptor and a donor site. Again in control-[Na][Cl], H-bonds shared among peptides account, on average, for $\sim$ 60% of the maximum achievable number, and water accounts for the rest, sharing H-bonds mainly with the extremal peptides A and E. Peptide-peptide H-bonds have nearly the same linear density (measured by the number of H-bonds per amino acid) along the peptide, with however a slight ($\sim$ 20%) decrease in the bend, compensated by a correspondingly higher linear density of peptide-water H-bonds in the same region.

The first effect of adding [Tea][Ms] to the solution is to decrease slightly the total number of H-bonds involving the protofibril, going from 75% capacity in control-[Na][Cl] to 70% in 25%-[Tea][Ms]. This change is caused primarily by a $\sim$ 20% loss in the number of peptide-peptide H-bonds, pointing to a relative destabilisation of the protofibril, and causing the observed decrease of the β-sheet character. Once again, the effects of [Tea][Ms] and [Tea][H_2PO_4] are similar, but a careful analysis of the H-bonding distribution among species shows characteristic differences. The most salt-specific effect consists of the sizeable number ($\sim$ 13 on average in 25%-[Tea][Ms]) of H-bonds donated by peptides to $[Ms]^-$. This concerns primarily peptide A, and to a lesser extent peptide E, while intermediate peptides are less affected. Moreover, most of these peptide-$[Ms]^-$ H-bonds are located at the bend and at β_2. Cooperativity in the H-bonding compensates this donation by an increase in the number of H-bonds accepted by peptides from water. Since, at the same time, the number of H-bonds accepted by water from peptides decreases, the net effect of [Tea][Ms] on water-peptide H-bonding is a modest enhancement, corresponding to a marginal salting-in of the protofibril when [Tea][Ms] is added. Despite its proton-donation ability, $[Tea]^+$ is virtually not involved in H-bonding to the protofibril. The changes of H-bonding in 26%-[Tea][H_2PO_4] with respect to control-[Na][Cl] are qualitatively the same to those of 25%-[Tea][Ms], but the H-bonding of peptides and anions is quantitatively less prominent. At the highest [Tea][Ms] concentration of 88%-[Tea][Ms], as expected, the number of protofibril-water H-bonds is significantly reduced, H-donation from peptide A and E to $[Ms]^-$ is sizeable, but the inter-peptide H-bonds are better conserved and better defined than at the lower RTIL concentration of 25%-[Tea][Ms].

X. STABILITY OF THE SALT BRIDGE

TABLE S4: Average number of intra-peptide salt bridges joining ASP8 to LYS13. nsb is the global average per peptide. nsbA to nsbE refer to the sub-average on peptide A to peptide E.

Sample	nsb	nsbA	nsbB	nsbC	nsbD	nsbE
control-[Na][Cl]	0.54	0.44	0.85	0.67	0.28	0.48
3%-[Tea][Ms]	0.66	0.38	0.95	0.84	0.71	0.40
11%-[Tea][Ms]	0.43	0.00	0.46	0.72	0.70	0.28
25%-[Tea][Ms]	0.42	0.15	0.55	0.12	0.30	0.99
88%-[Tea][Ms]	0.75	0.63	0.88	0.58	0.99	0.66
26%-[Tea][H_2PO_4]	0.46	0.02	0.62	0.86	0.54	0.27

XI. HYDRATION OF THE SALT BRIDGE

TABLE S5: Average number of H-bonds donated by water to the two terminal oxygens of ASP8, which is part of the first hydration shell of the salt bridge. As in the previous table, nH is the total of the nHA, ..., nHE contributions from each peptide.

Sample	nH	nHA	nHB	nHC	nHD	nHE
control-[Na][Cl]	10.91	2.65	0.77	1.17	1.90	4.42
3%-[Tea][Ms]	11.28	3.92	0.51	1.05	1.64	4.16
11%-[Tea][Ms]	11.83	4.22	1.36	1.05	1.27	3.92
25%-[Tea][Ms]	10.69	1.95	1.58	2.13	1.80	3.24
88%-[Tea][Ms]	7.37	0.86	1.85	1.02	1.32	2.32
26%-[Tea][H_2PO_4]	12.2	2.97	1.56	1.21	2.41	4.05

TABLE S6: Average number of H-bonds donated by the NH3 termination of LYS 13 to OW, which is part of the first hydration shell of the salt bridge. As in the previous two tables, nH is the total of the nHA, ..., nHE contributions from each peptide.

Sample	nH	nHA	nHB	nHC	nHD	nHE
control-[Na][Cl]	4.15	1.55	0.53	0.61	0.57	0.89
3%-[Tea][Ms]	4.45	1.60	1.00	0.52	0.40	0.93
11%-[Tea][Ms]	5.05	1.72	1.69	0.47	0.40	0.79
25%-[Tea][Ms]	4.32	1.85	0.40	0.71	1.16	0.19
88%-[Tea][Ms]	3.52	1.70	0.65	0.43	0.68	0.05
26%-[Tea][H_2PO_4]	3.56	0.72	0.92	0.66	0.70	0.56

XII. STEERED MD SIMULATIONS

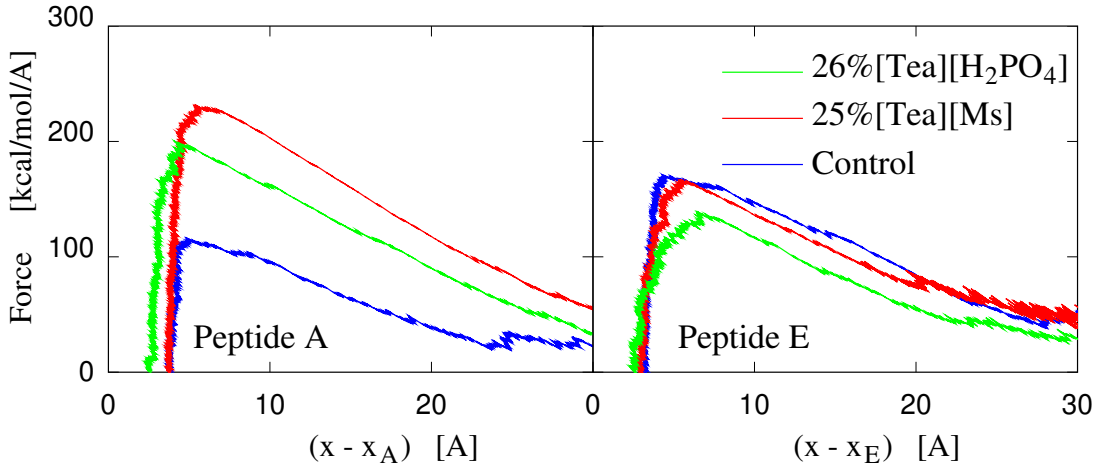

FIG. S9: Force versus distance relation for the pulling of peptide A or peptide E away from the remaining four peptide, determined during the steered MD stage of the free energy computation.

XIII. STRUCTURAL AND H-BONDING PROPERTIES OF SINGLE β(17-42) PEPTIDES IN SOLUTION

The simplest characterisation of a polymer in solution is given by the probability distribution $P(r_{ee})$ for the distance r_{ee} between the first and the last (end-to-end) polymer bead. If a is the separation of consecutive beads along a polymer N-beads long, the relation $\langle r_{ee}\rangle = \int uP(u)du < a\sqrt{N}$ identifies poor solvent conditions, at which the polymer is collapsed, while $\langle r_{ee}\rangle > a\sqrt{N}$ corresponds to *good solvent* conditions, at which the polymer is expanded. In our simulations (see Tab. S7), the peptide in the control sample and in 25%-[Tea][Ms] has almost exactly $\langle r_{ee}\rangle = a\sqrt{N} = 3.83\sqrt{27} = 19.9$ Å , which identifies the so-called theta-point condition, at which attractive and repulsive interactions between beads and solvent compensate each other and the polymer behaves like an ideal chain. According to the data in Tab. S7, the peptide in 88%-[Tea][Ms] and in 26%-[Tea][H_2PO_4] is collapsed, pointing to the prevalence of hydrophobic interactions, causing the salting out of the peptide. In these cases, however, salting out might not uniquely correspond to the stabilisation of the single peptide, for the reasons discussed below. Of course one cannot expect that plain MD simulations on the 10^2 ns scale will recover the equilibrium folding of the peptide, but the persistence of the same overall configuration during the last 40 ns of the production stage after a long equilibration and many isomerisations suggests that the system has reached a state of relatively low free energy.

Because of the role of atomic charges and H-bonds, however, peptides in solution are more complex than simple polymers, especially in the short-chain limit, far from universality. Computation of the principal radii of the approximating ellipsoid, for instance, shows that only in control-[Na][Cl] the peptide is relatively globular, approaching an isotropic ratio of the principal radii a, b and c. In 25%-[Tea][Ms], 88%-[Tea][Ms] and 26%-[Tea][H_2PO_4], instead, one dimension of the approximating ellipsoid is much longer than the other two ($c >> a \sim b$), tending to a prolate ellipsoid geometry. The persistent anisotropy shows that in these samples the peptide, although apparently more flexible than the protofibril, is still able to keep a shape not purely determined by entropy considerations. Estimating the volume of the peptide assuming again that it is an ellipsoid of homogeneous density, one finds that in control-[Na][Cl] it assumes the most compressed configuration, in 25%-

TABLE S7: Structural and H-bonding properties of Aβ(17-42) single peptide in solution. a, b and c are the principal radii of the ellipsoid approximating the peptide shape. $Vol = 4\pi abc/3$. W_α and W_β weights are defined in the main text. The arrow in the rows concerning H-bonding indicates the direction of the proton donation. Number of significant digits compatible with the error bar. Only H-bonds involving backbone atoms are counted.

Single peptide	control-[Na][Cl]	25%-[Tea][Ms]	88%-[Tea][Ms]	26%-[Tea][H_2PO_4]
end-to-end Å	20.7	18.3	13.1	9.3
a Å	7.1	8.3	6.5	7.3
b Å	10.4	9.6	11.5	9.3
c Å	12.5	16.0	21.7	15.7
Vol Å ^{3}	3860	5340	6770	4710
$W_\beta(\beta_1)$	0.85	0.56	0.97	0.87
$W_\beta(\beta_2)$	0.67	0.68	0.64	0.60
$W_\alpha(\beta_1)$	0.14	0.29	0.00	0.13
$W_\alpha(\beta_2)$	0.23	0.18	0.28	0.22
$W_\alpha(bend)$	0.08	0.51	0.50	0.00
HB intra-peptide	7.61	1.69	0.28	5.20
Salt bridge	0	0	0	0
HB Wat→ Peptide	14.0	12.3	5.8	10.6
HB Peptide → Water	6.4	3.4	2.4	5.0
Cation → Peptide	0.0	0.6	0.9	0.1
Peptide → Anion	0	8.6	13.8	3.8

[Tea][Ms] and 88%-[Tea][Ms] the most expanded one, with 26%-[Tea][H_2PO_4] in between control-[Na][Cl] and 25%-[Tea][Ms], in only partial agreement with the ordering provided by the computation of $\langle r_{ee} \rangle$. The results of several other analyses provide the same alternation of contrasting results, emphasising the complexity of peptides' behaviour in solution.

XIV. STRUCTURAL AND H-BONDING PROPERTIES OF β(17-42) PEPTIDE PAIRS IN SOLUTION

TABLE S8: Structural and H-bonding properties of Aβ(17-42) peptide pairs in solution. a, b and c are the principal radii of the ellipsoid approximating the peptide pair shape. $Vol = 4\pi abc/3$. W_α and W_β weights are defined in the main text. The arrow in the rows concerning H-bonding indicates the direction of the proton donation. Only H-bonds involving backbone atoms are counted. Number of significant digits compatible with the error bar.

Peptide dimer	control-[Na][Cl]	25%-[Tea][Ms]	88%-[Tea][Ms]	26%-[Tea][H_2PO_4]
a Å	8.4	6.9	6.1	8.4
b Å	11.5	13.6	12.4	12.5
c Å	20.2	23.0	24.8	22.7
Vol Å ^{3}	8120	9120	7820	9975
$W_\beta(\beta_1)$	0.99	0.95	0.99	0.99
$W_\beta(\beta_2)$	0.81	0.78	0.75	0.72
$W_\alpha(\beta_1)$	0.	0.02	0	0
$W_\alpha(\beta_2)$	0.10	0.05	0.04	0.10
$W_\alpha(bend)$	0.19	0.28	0.17	0.39
Intra-Peptide	2.6	0.2	0.2	0.1
Salt bridge	0	0.4	0.8	0.1
Peptide A $\rightarrow$ Peptide B	7.4	8.	8.8	7.1
Peptide B $\rightarrow$ Peptide A	6.5	7.8	9.7	7.6
HB Water $\rightarrow$ Peptide	27.4	20.8	9.5	22.0
HB Peptide $\rightarrow$ Water	10.1	7.5	5.8	11.6
Cation $\rightarrow$ Peptide	0	0.8	2.0	0.1
Peptide $\rightarrow$ Anion	0	8.9	12.7	6.2

[1] CPMD, http://www.cpmd.org/, Copyright IBM Corp 1990-2015, Copyright MPI für Festkörperforschung Stuttgart 1997-2001.

[2] Troullier,N.; Martins, J. L. Efficient pseudopotentials for plane-wave calculations. *Phys. Rev. B* **1991**, *43*, 1993-2006.

[3] Perdew, J. P.; Burke, K.; Ernzerhof, M. Generalized gradient approximation made simple. *Phys. Rev. Lett.* **1996**, *77*, 3865-3868.

[4] Barnett, R. N.; Landman, U. Born-Oppenheimer molecular-dynamics simulations of finite systems: Structure and dynamics of $(H_2O)_2$. *Phys. Rev. B* **1993**, it 48, 2081-2097.

[5] Yang, Z. Hofmeister effects: an explanation for the impact of ionic liquids on biocatalysis. *J. Biotechnol.* **2009**, *144*, 12-22.

[6] Debeljuh, N.; Barrow, C. J.; Byrne, N. The impact of ionic liquids on amyloid fibrillation of Aβ16-22: tuning the rate of fibrillation using a reverse Hofmeister strategy. *Phys. Chem. Chem. Phys.* **2011**, *13*, 16534-16536.

[7] Thomas, A. S.; Elcock, A. H. Molecular dynamics simulations of hydrophobic associations in aqueous salt solutions indicate a connection between water hydrogen bonding and the Hofmeister effect. *J. Am. Chem. Soc.* **2007**, 14887-14898.